

Earth's surface movements in relation to Parkfield 2004 earthquake: Interpretation of permanent GPS observations

V. I. Kaftan, R. I. Krasnoperov

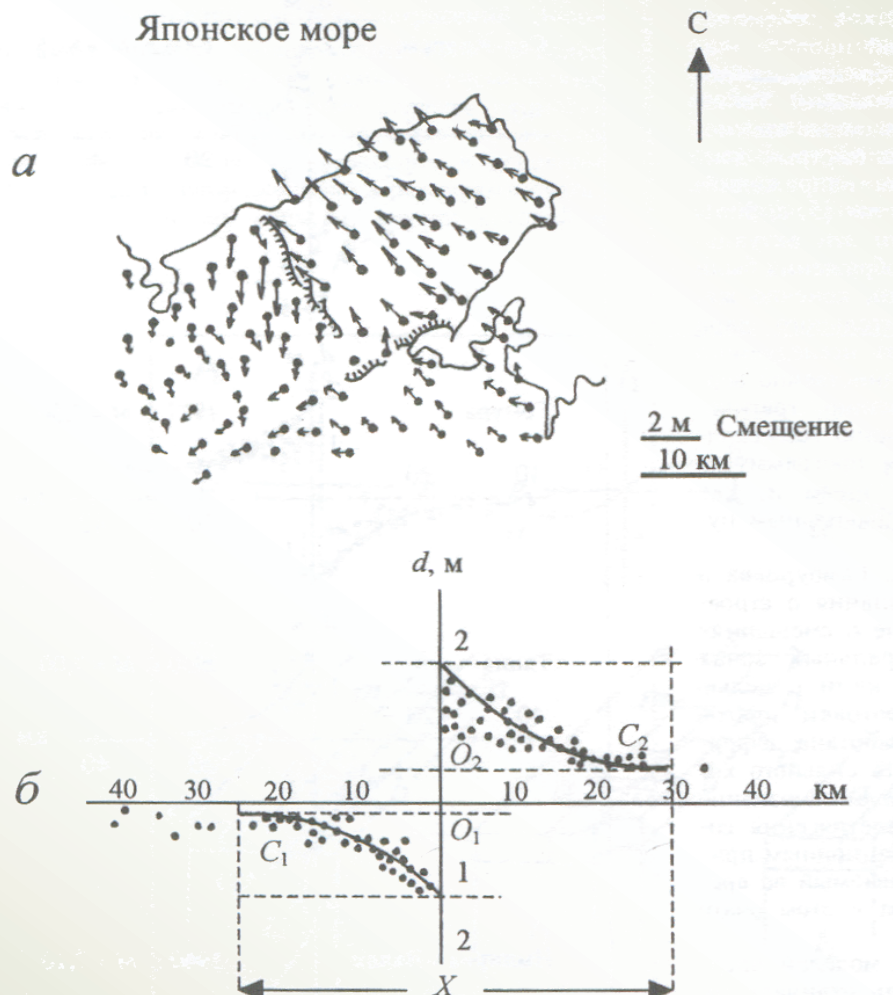
IAG Scientific Assembly, Potsdam, September 1-6, 2013

Age-long history of elastic rebound model

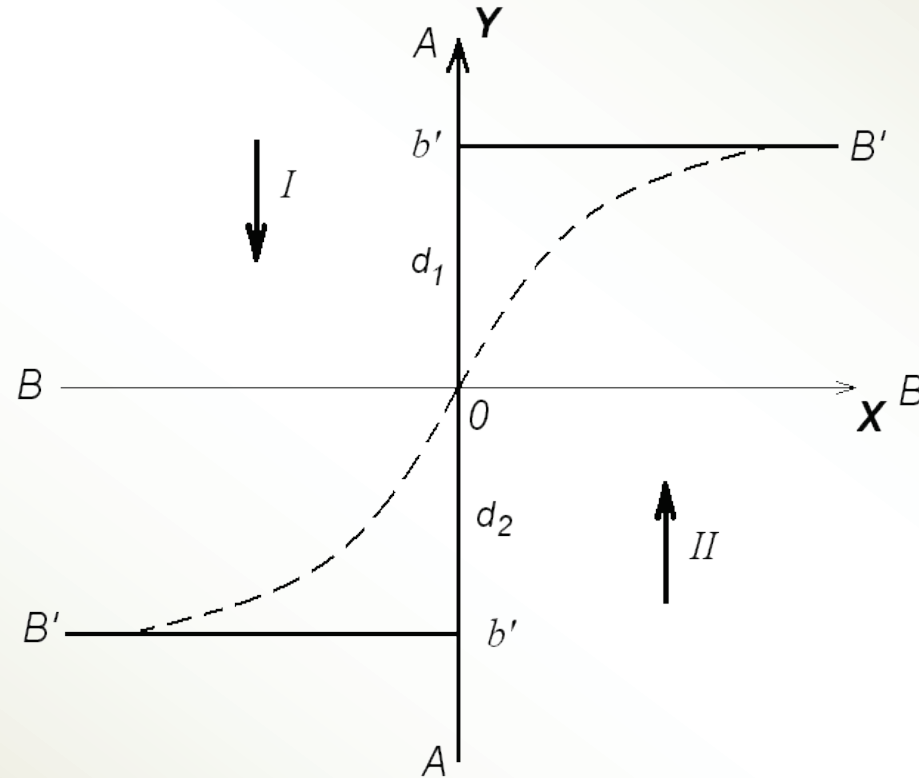
- San Francisco earthquake, April 18, 1906, M=7.9,
- Reid, H.F., The Mechanics of the Earthquake, The California Earthquake of April 18, 1906, Report of the State Investigation Commission, Vol.2, Carnegie Institution of Washington, Washington, D.C. **1910**
- Kanamori H. Mode of strain release associated with major earthquake in Japan / In: Donath F.A. (editor) Annual Review of Earth and Planetary Sciences, Annual Reviews, Palo Alto, Calif. – 1972.- 1.- 213
- Pevnev A. K. , “Earthquake prediction: geodetic aspects of the problem,” Izvestiya, Physics of the Solid Earth, vol. 12, pp. 88–98, 1988.



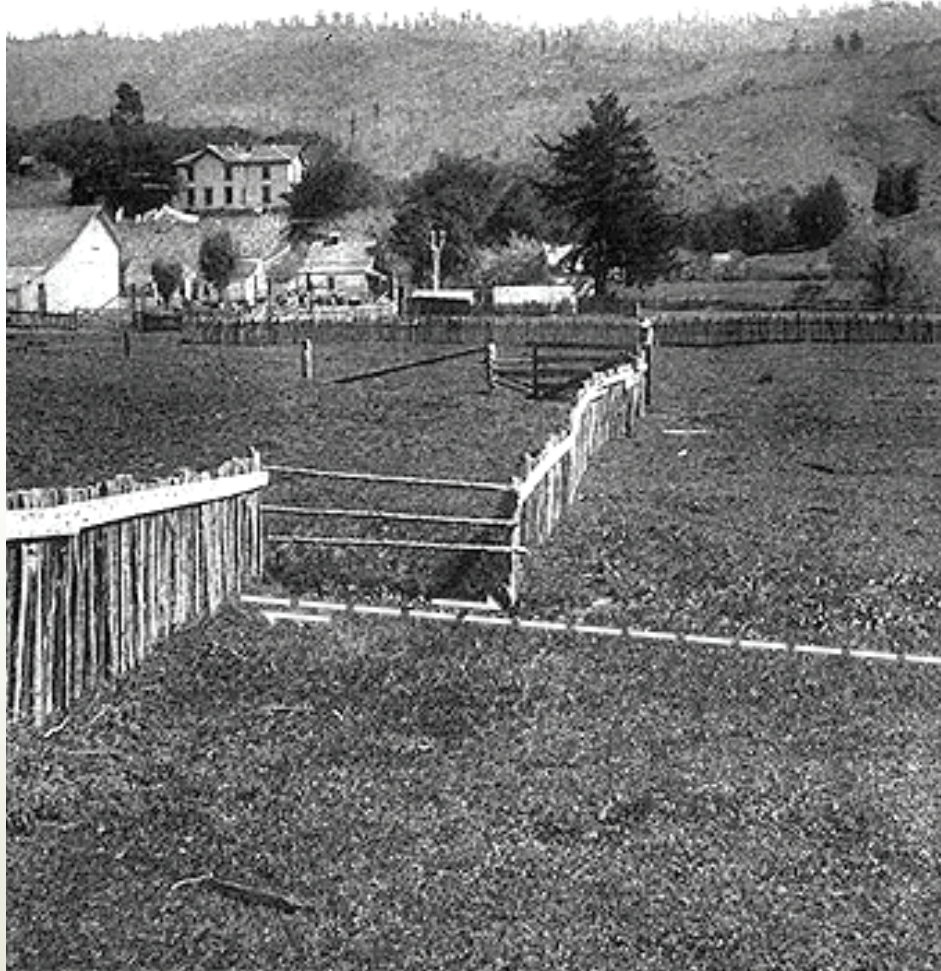
Classical model example of Tango earthquake (Japan, 1927, M=7.5)



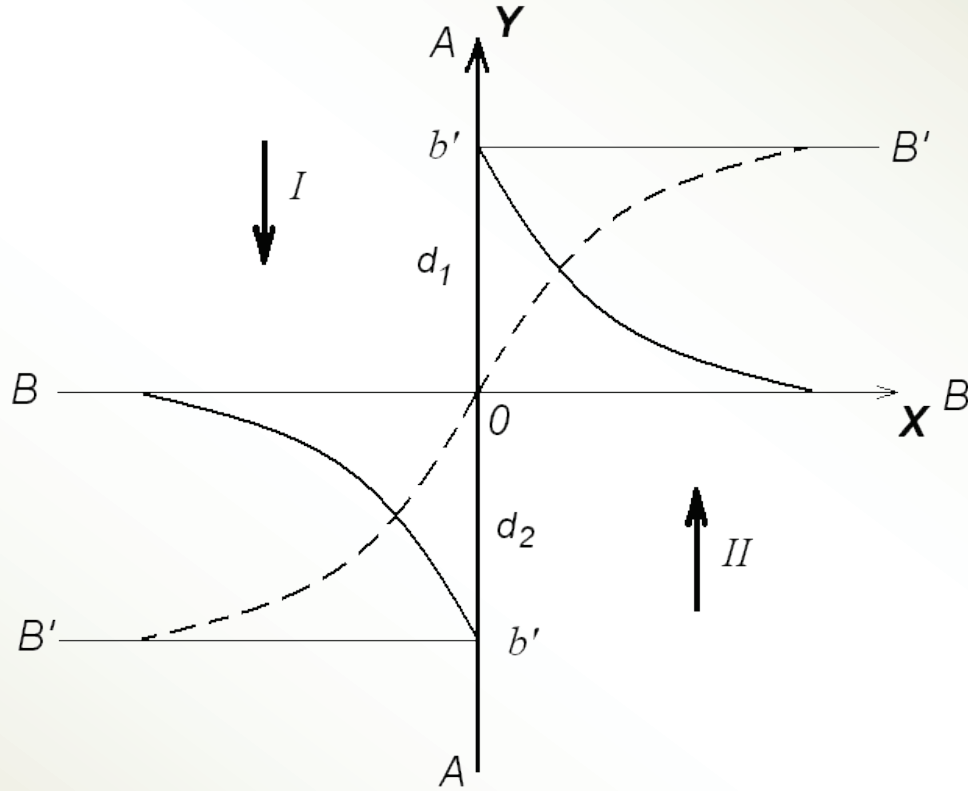
Elastic rebound (case 1: first epoch at the beginning of elastic strains)



The fence on the San Andreas (by G.K. Gilbert from Steinbrugge Collection of the UC Berkeley Earthquake Engineering Research Center)

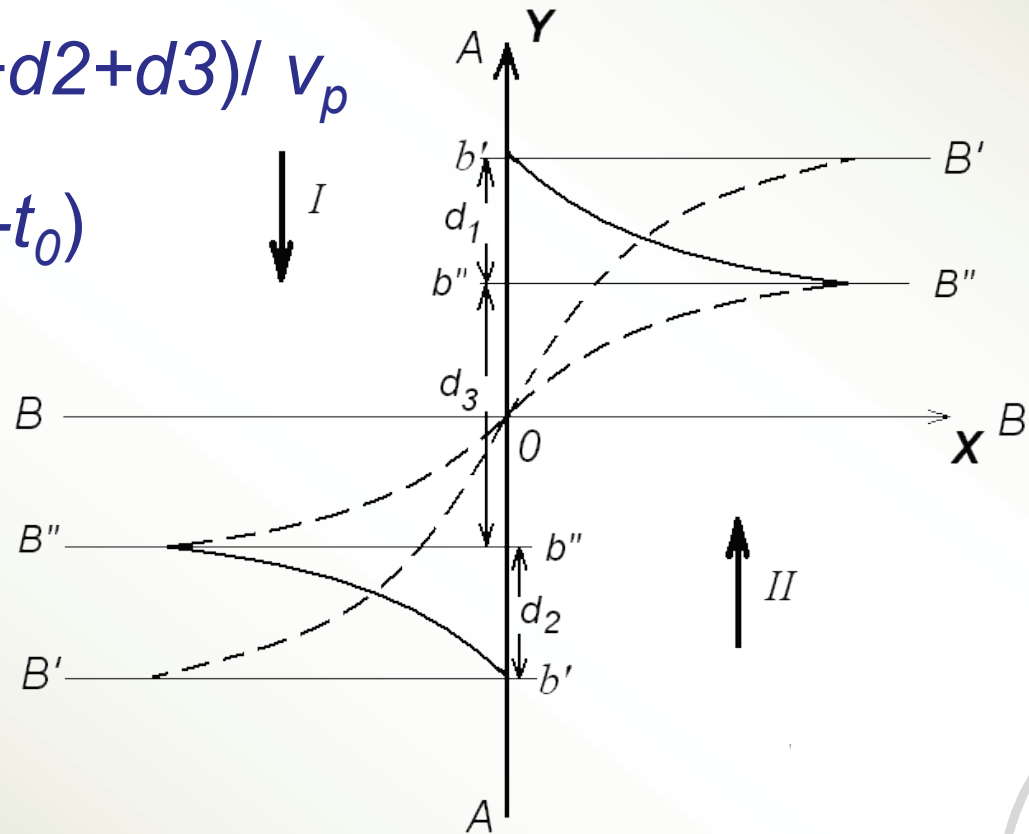


Elastic rebound (case 2: first epoch a day before the earthquake)

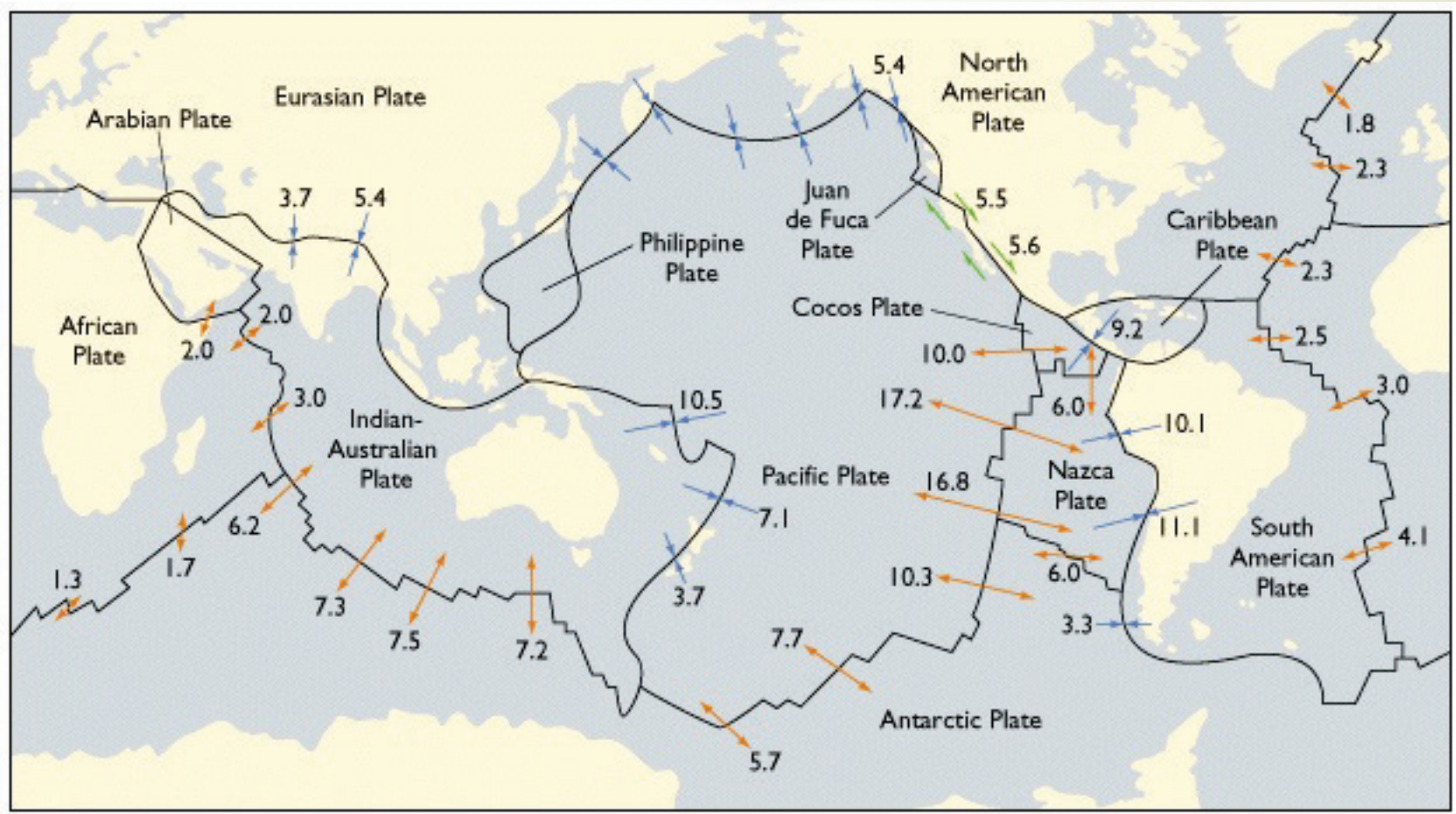


Elastic rebound (common case 3: first epoch at the deformed surface)

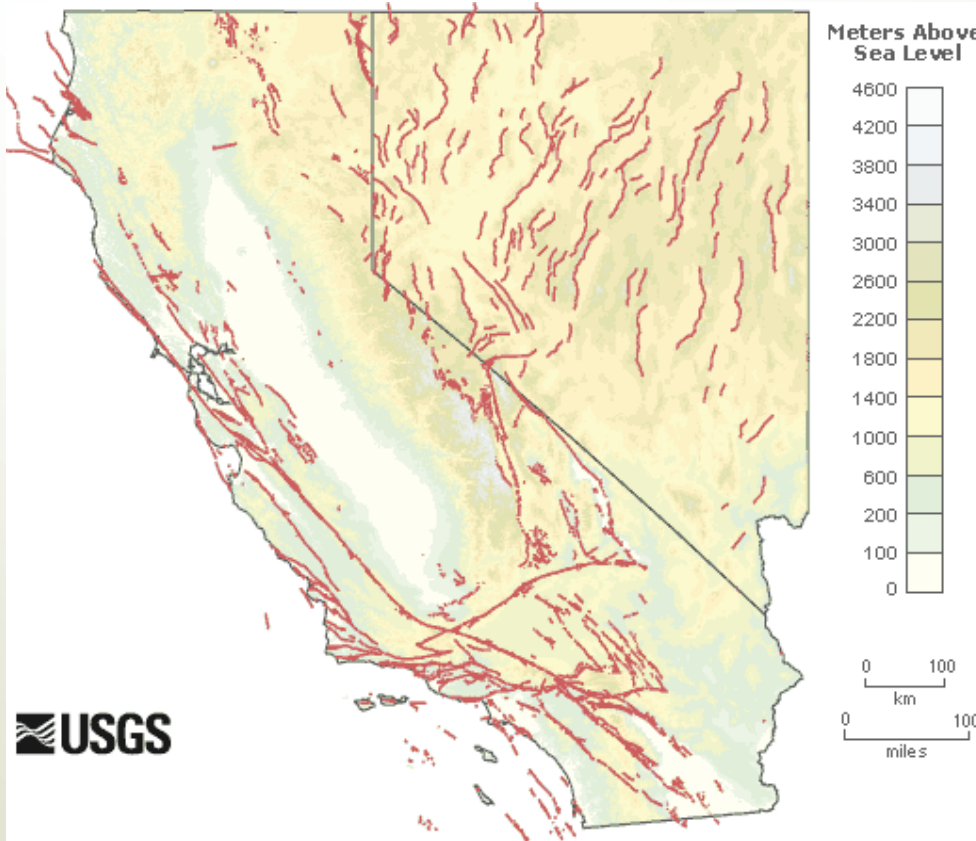
- $T_p = (d_1 + d_2 + d_3) / v_p$
- $v_p = d_3 / (t_i - t_0)$



The lithospheric plate boundaries are of three types:
Divergent, Convergent, Transform.
The model more usable to the last one



Investigated region



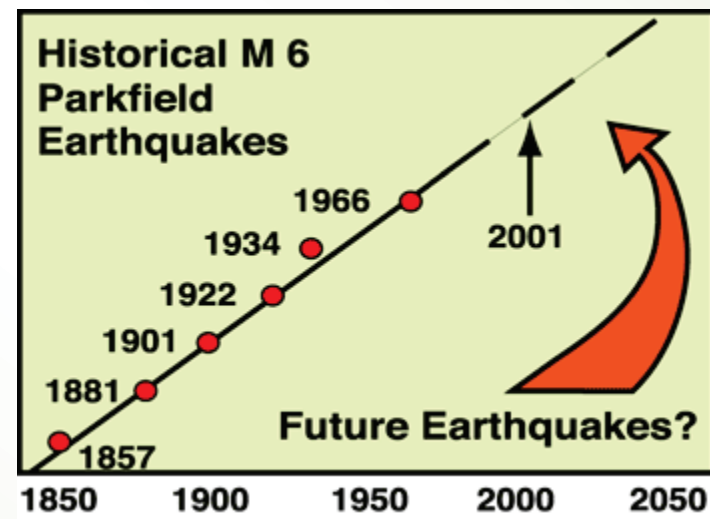
Tectonic fault map (California, USA)



San Andreas fault (California, USA)

Parkfield prediction experiment. California Integrated Seismic Network.

- Long term prediction for the strong earthquake moment was 1985-1993
- Prediction was based on about regular earthquake repeatability
- Place was predicted accurately



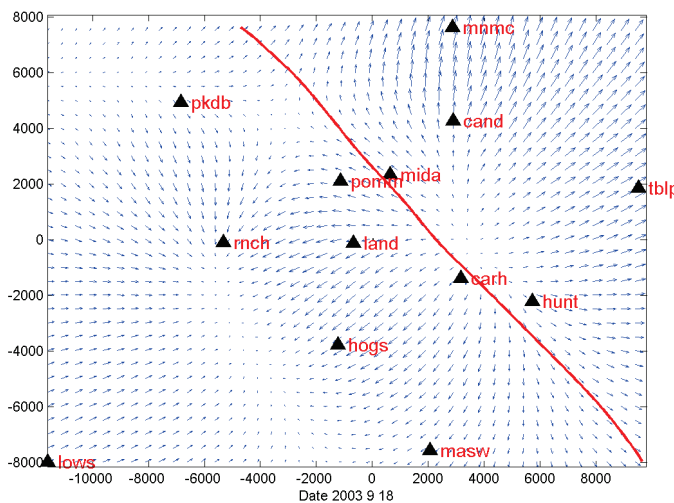
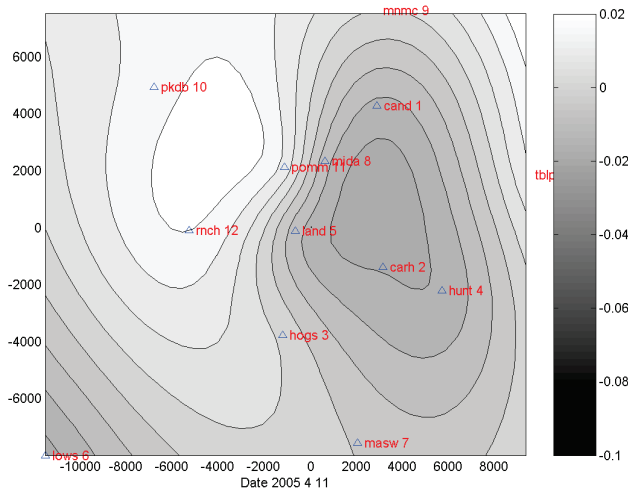
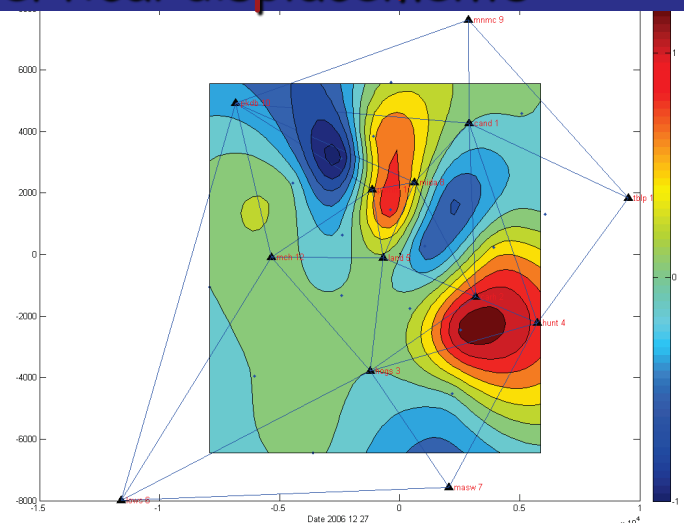
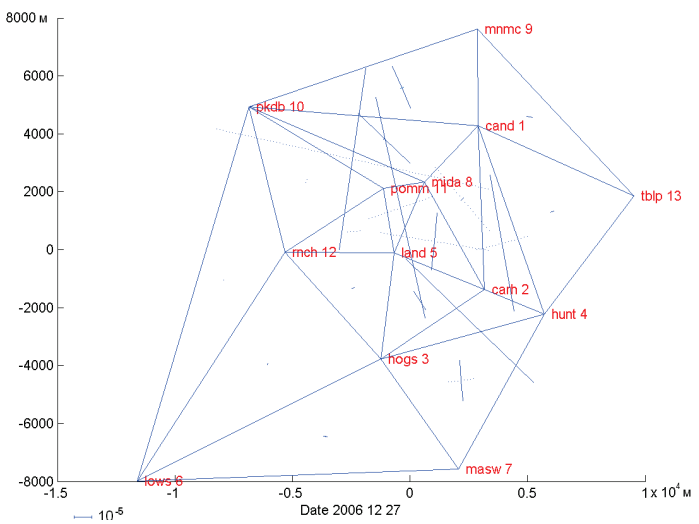
GPS network specification

Number of points:	13
Number of selected baselines:	30
Baseline lengths:	1—14 km
Organization:	PBO (Plate Boundary Observatory)
Measurement mode:	permanent

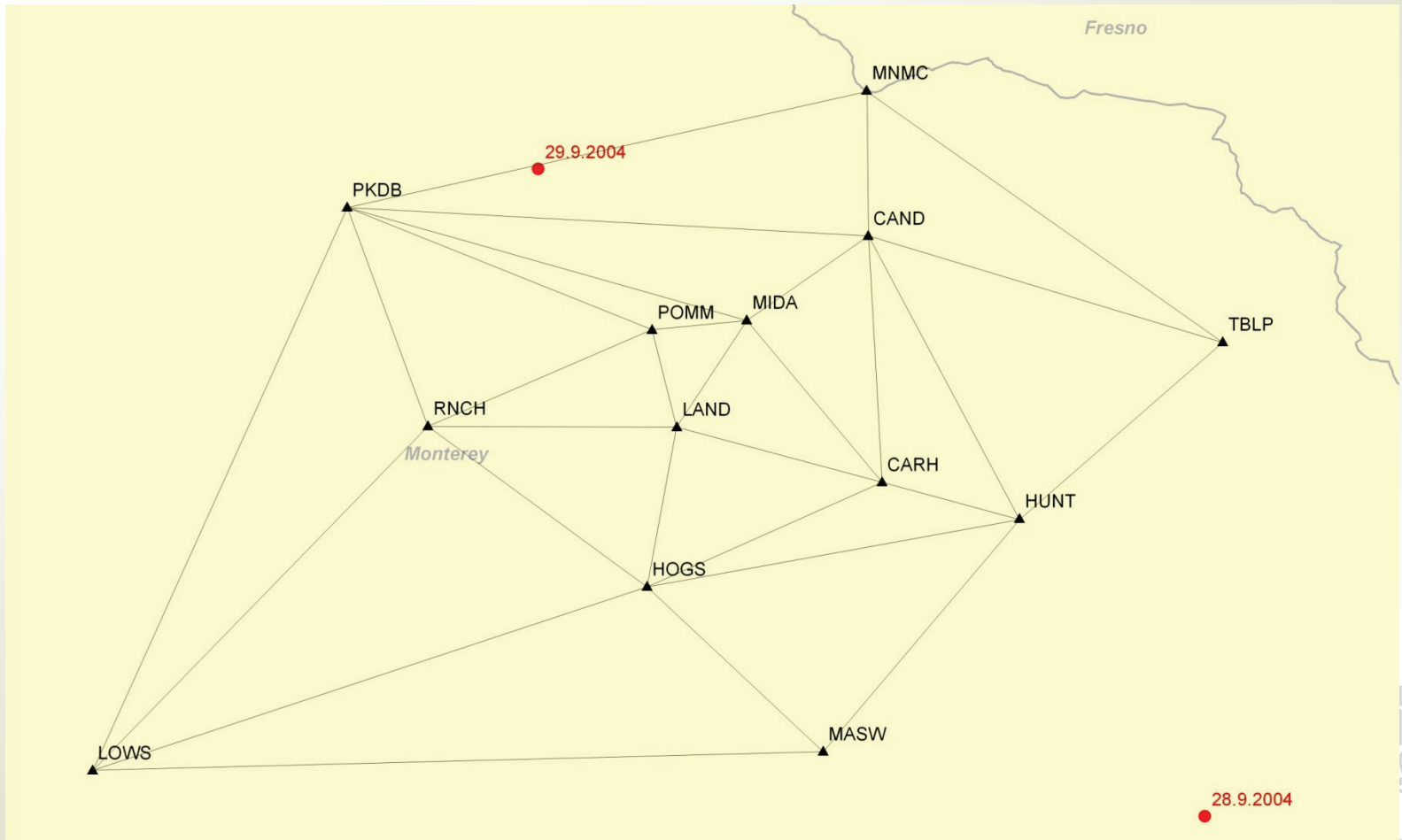


Received deformation:

1) Main deformation axes, 2) Dilatation, 3) Vertical displacements,
4) Horizontal gradients of vertical displacements



PBO GPS network (Parkfield experiment tool)



Main Parkfield earthquake epicenters, September 28-29 2004 (M 6.0 and 5.1)

Measurement results received

- SOPAC archive data was used for baseline processing
- Used date interval: 01.01.2002—27.12.2006
- Number of processed epochs: 365
- Interval between epochs: 5d
- Used software: Topcon Tools v. 7.1



Earth crust movement and deformation analysis

- Initial data:
 - Baseline vectors
 - Covariance matrixes
- Data processing (the special software was made and used)
 - Temporal difference baseline components computation
 - Covariance matrix determination
 - Especial adjustment for determination of point displacements

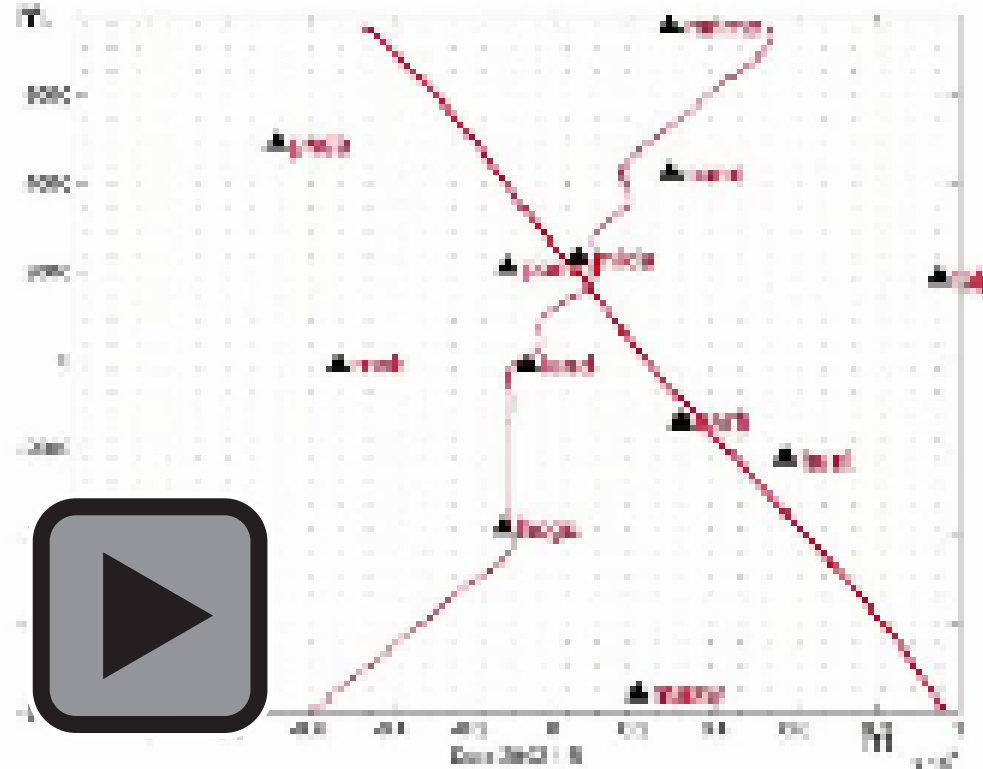


Earth crust movement and deformation analysis

- Deformation analysis
 - Transformation to a local reference system (NEU)
 - Deformation component computation
 - Accuracy estimation
- Graphic and animation representation

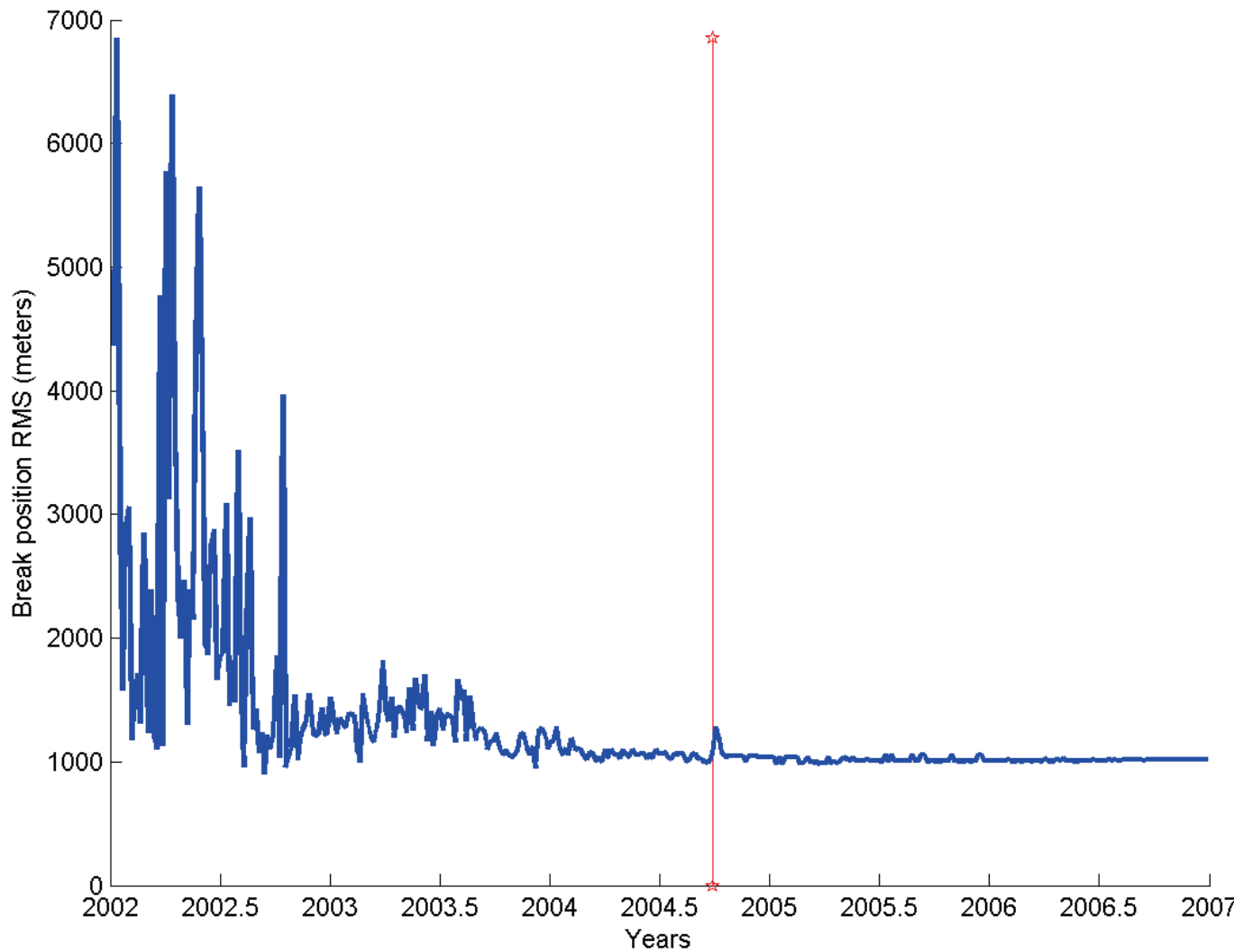


Horizontal displacements (digital model)

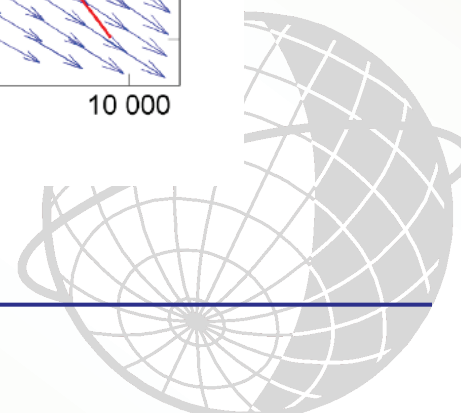
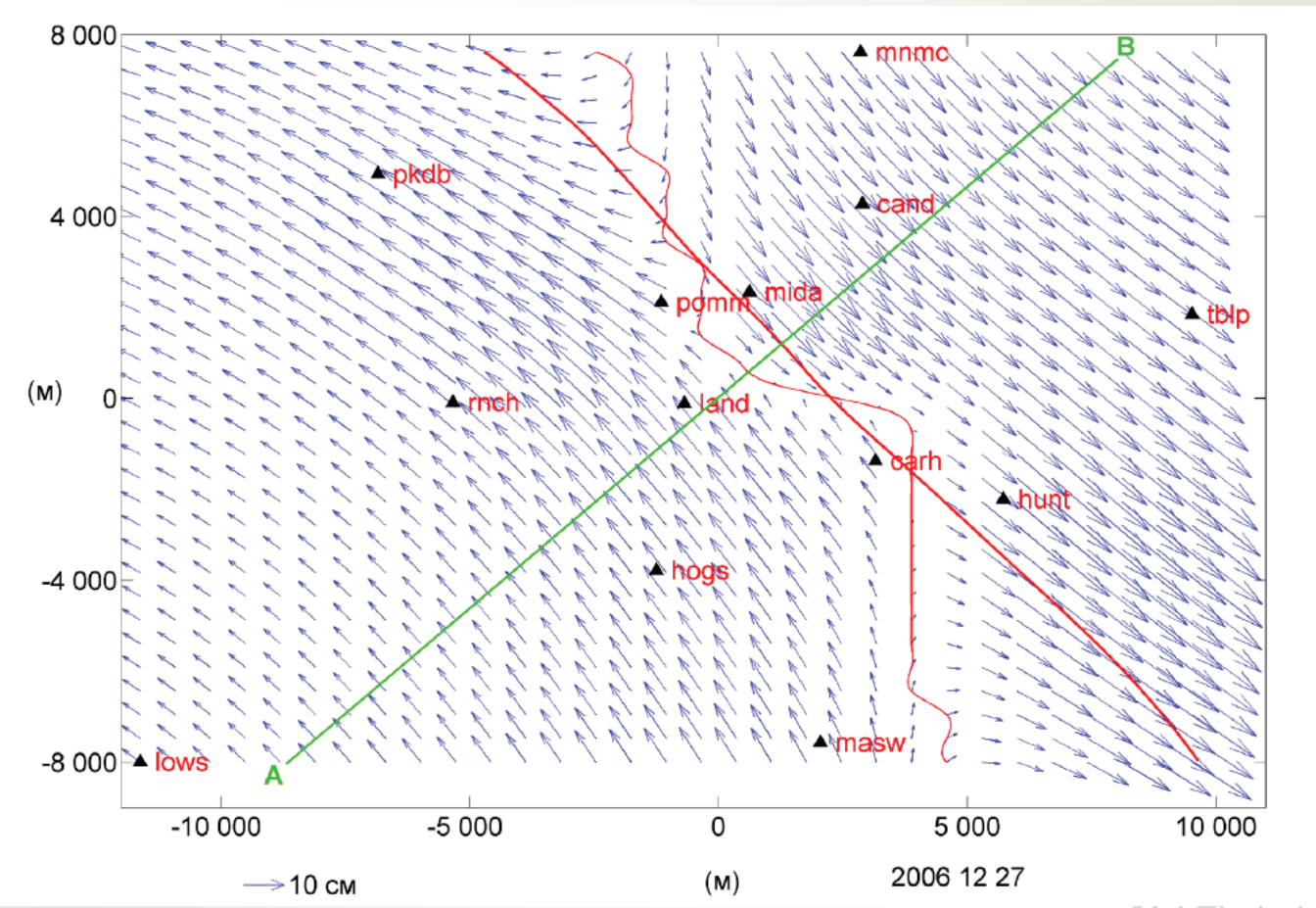


Solid red line - actual fault
Thin red line - rupture model line

Rupture position RMS

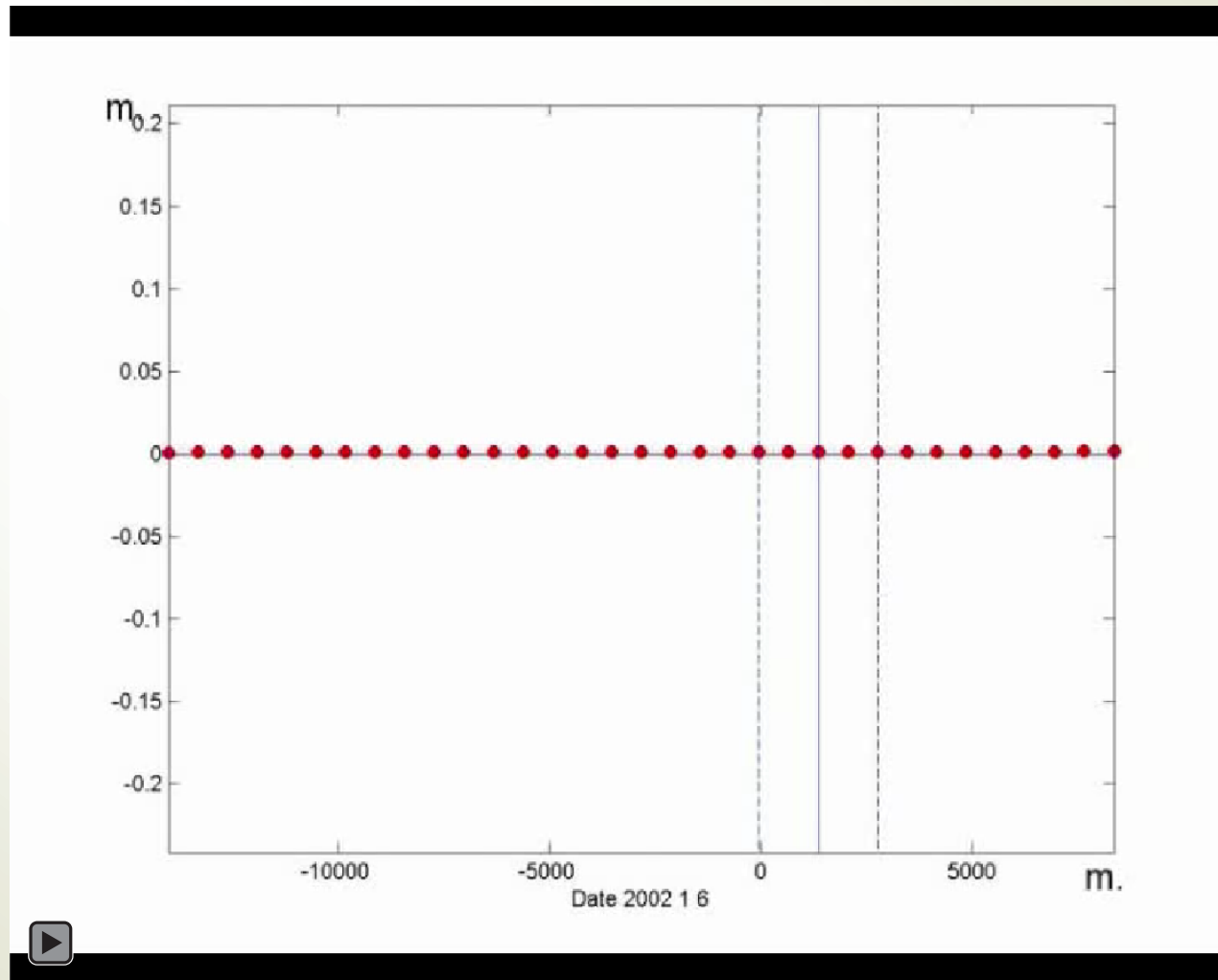


Elastic rebound test cross-section



Elastic rebound animation

Fault zone



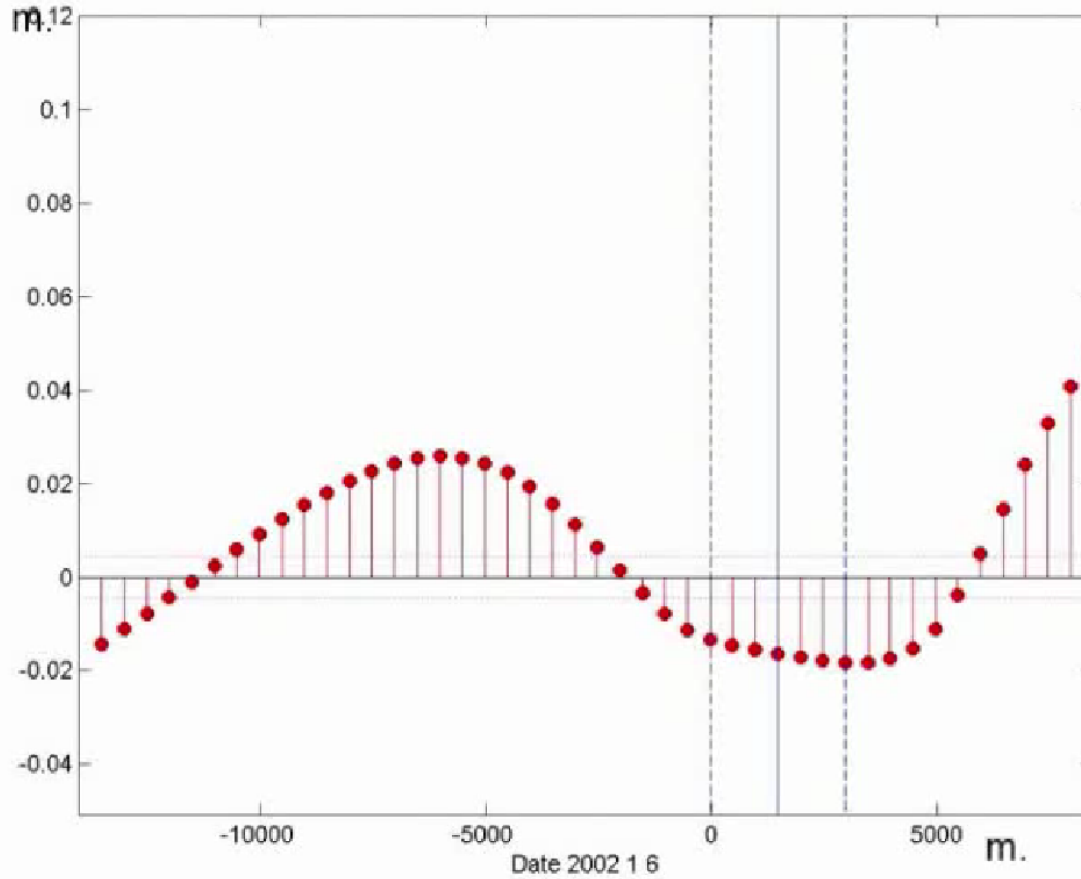
Computation of strain accumulation start moment

- $t = 2.74 \text{ yr}$
- $dN_i - dN_j = 42.5 \text{ cm}$
- $dN'_i - dN'_j = 3.5 \text{ cm}$
- $T = (dN_i - dN_j)t / (dN'_i - dN'_j) = 33 \pm 7 \text{ yr}$
- Elastic strain accumulation has begun at 1972 ± 7 just after the previous earthquake of 1966

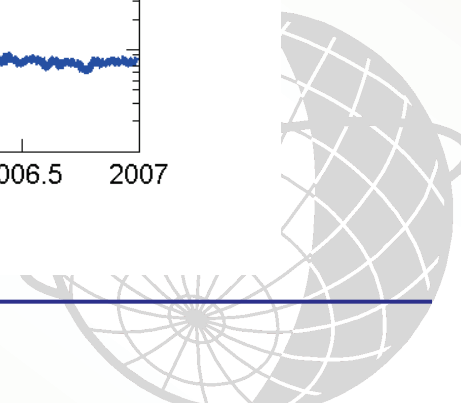
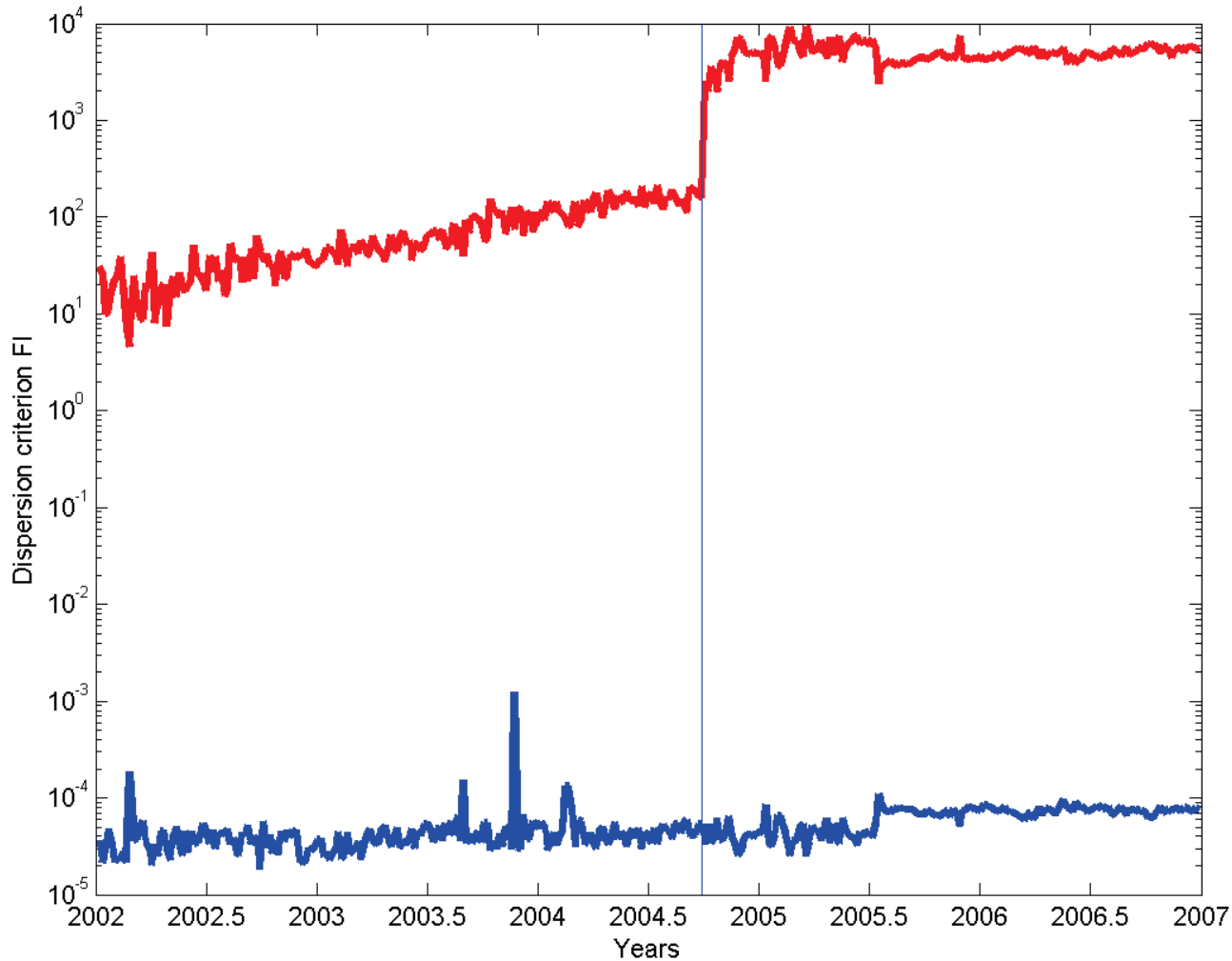


Vertical displacements across the fault

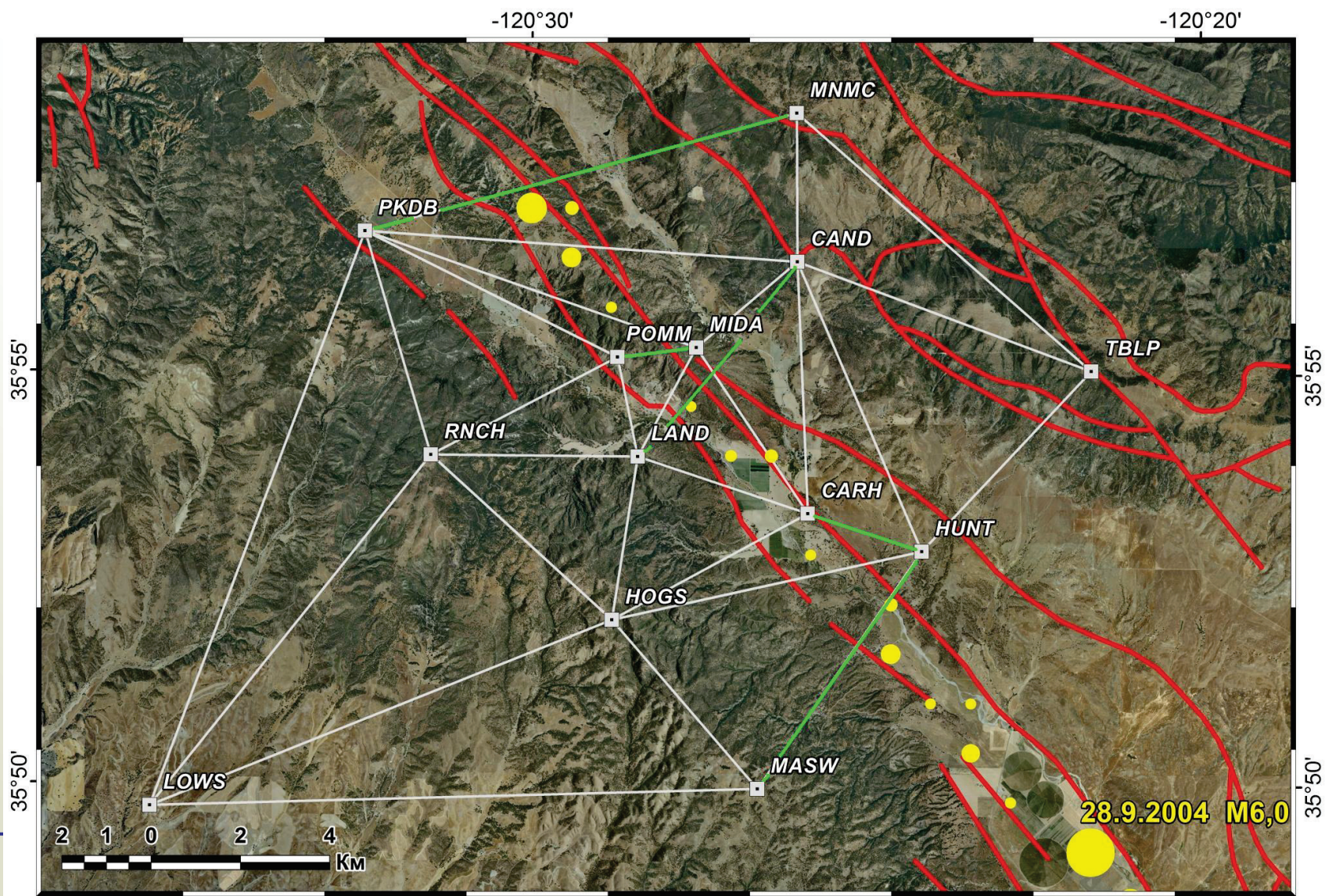
Fault zone



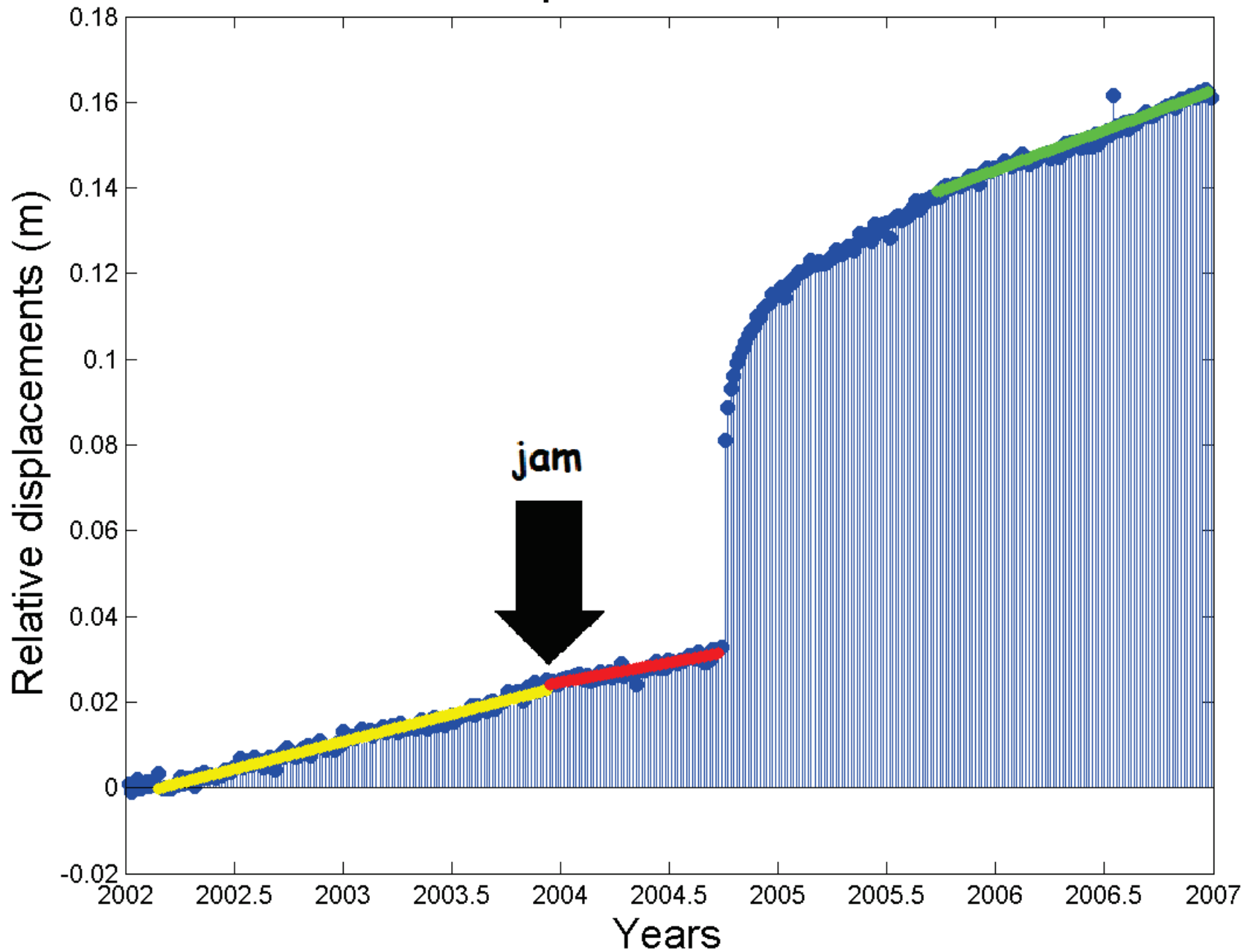
Global deformation test



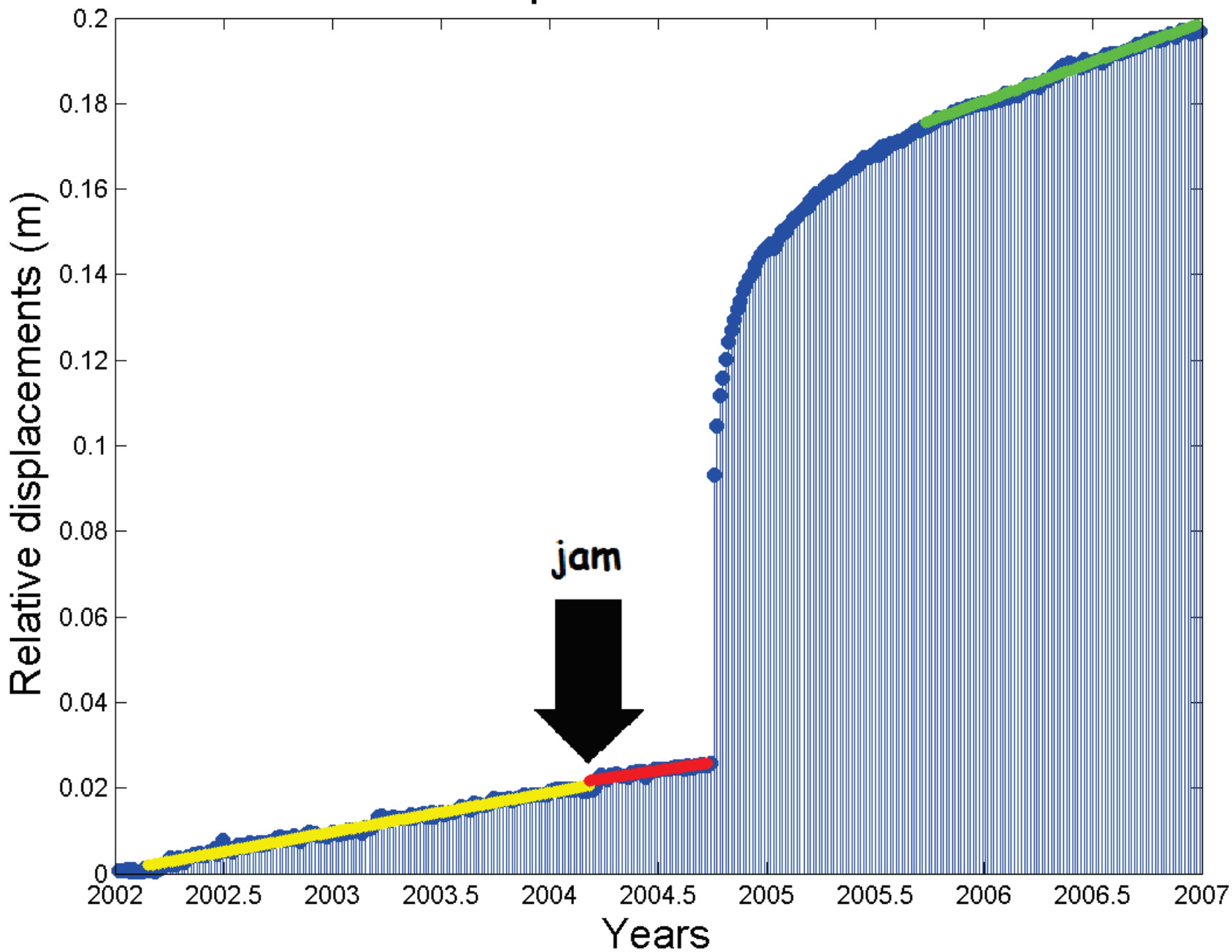
Creep velocity comparison mowing to epicentre



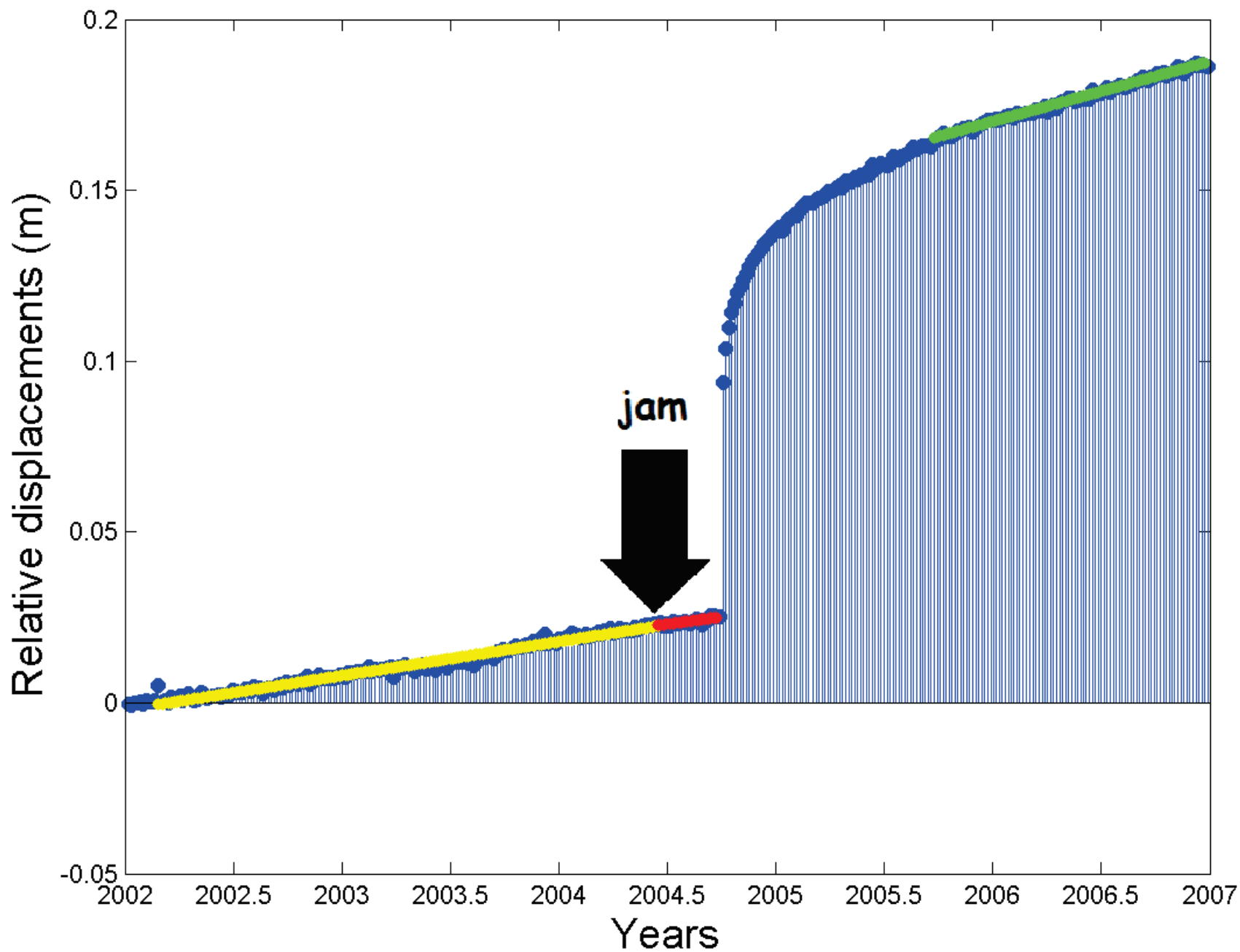
pkdb-mnmc



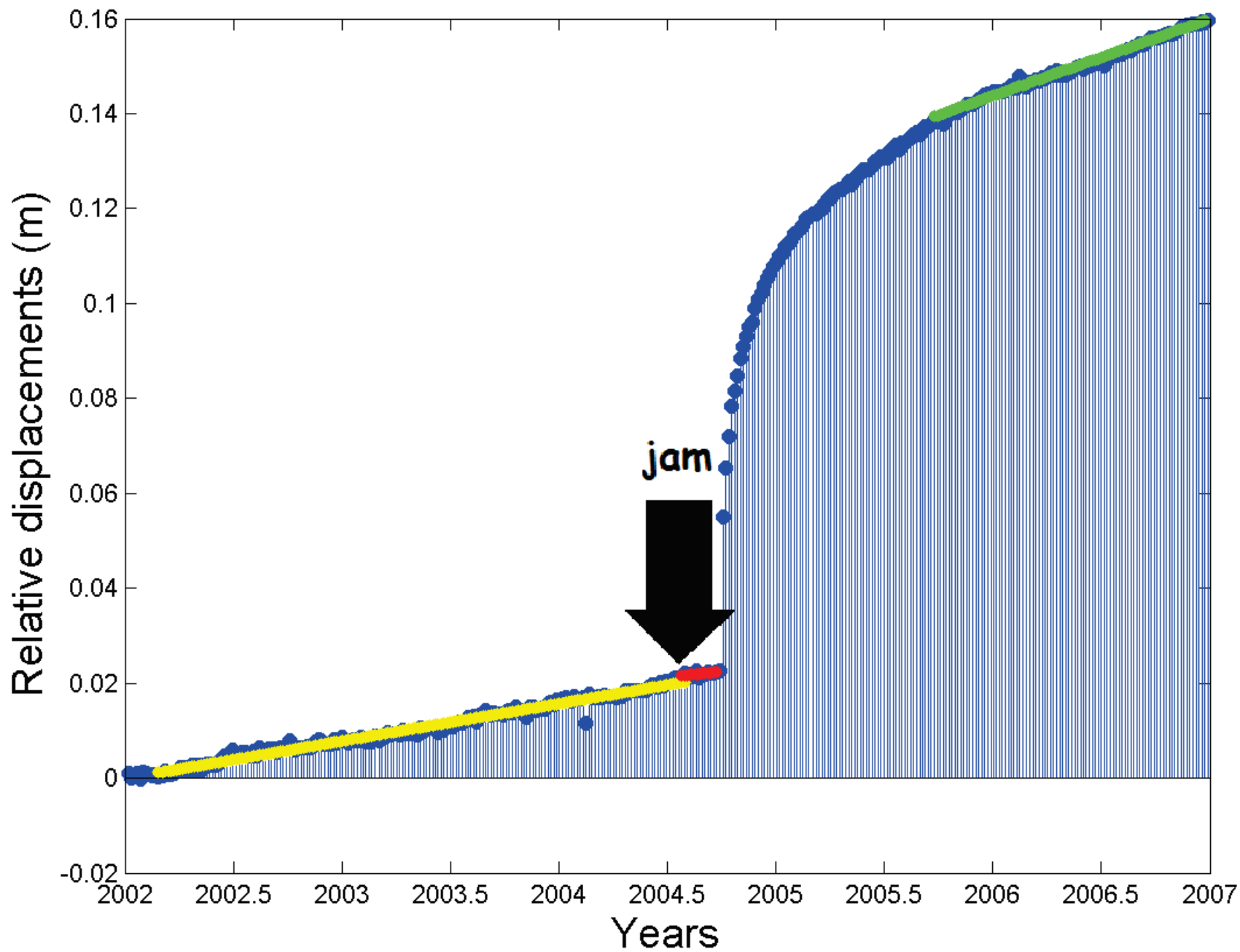
pomm-mida



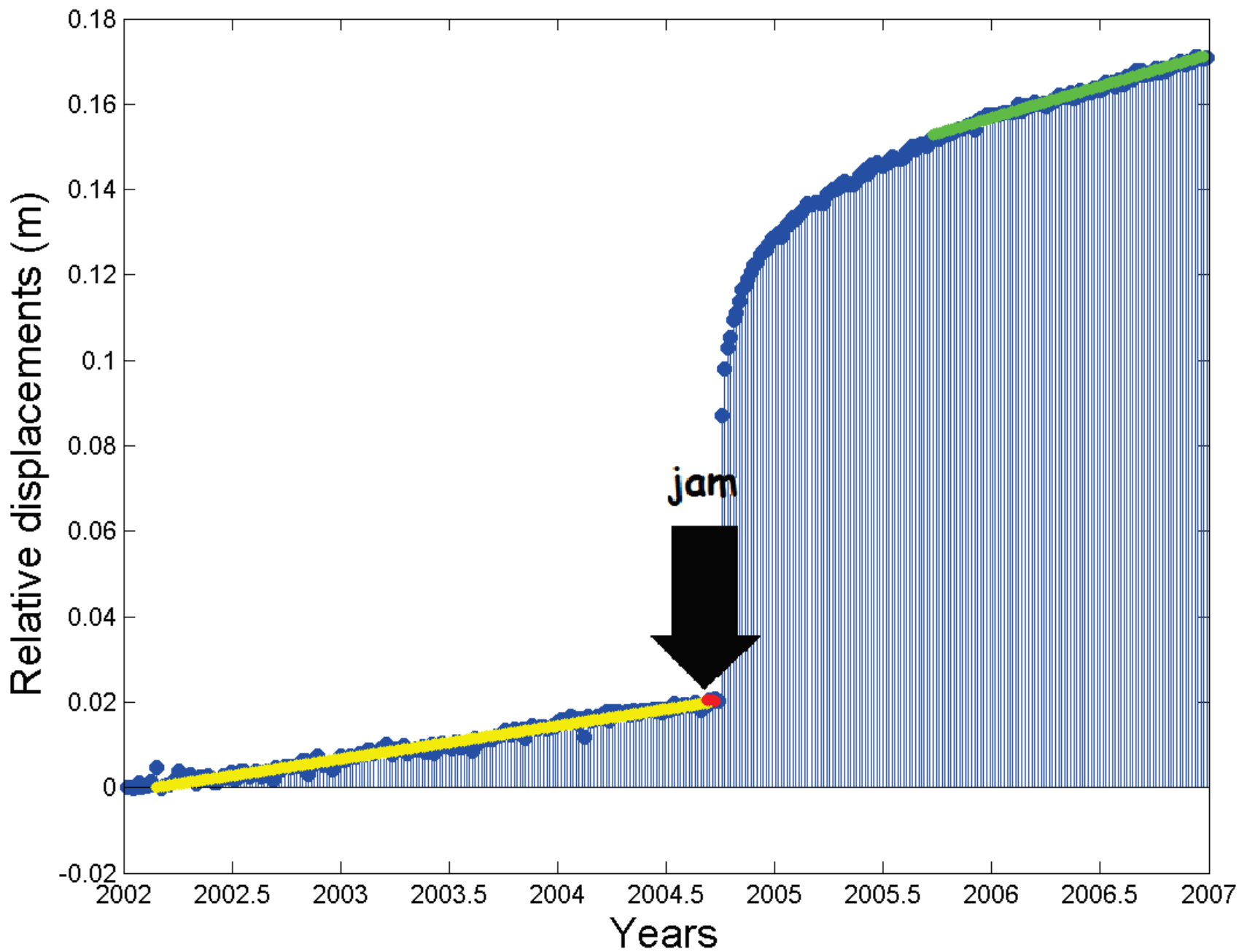
land-cand



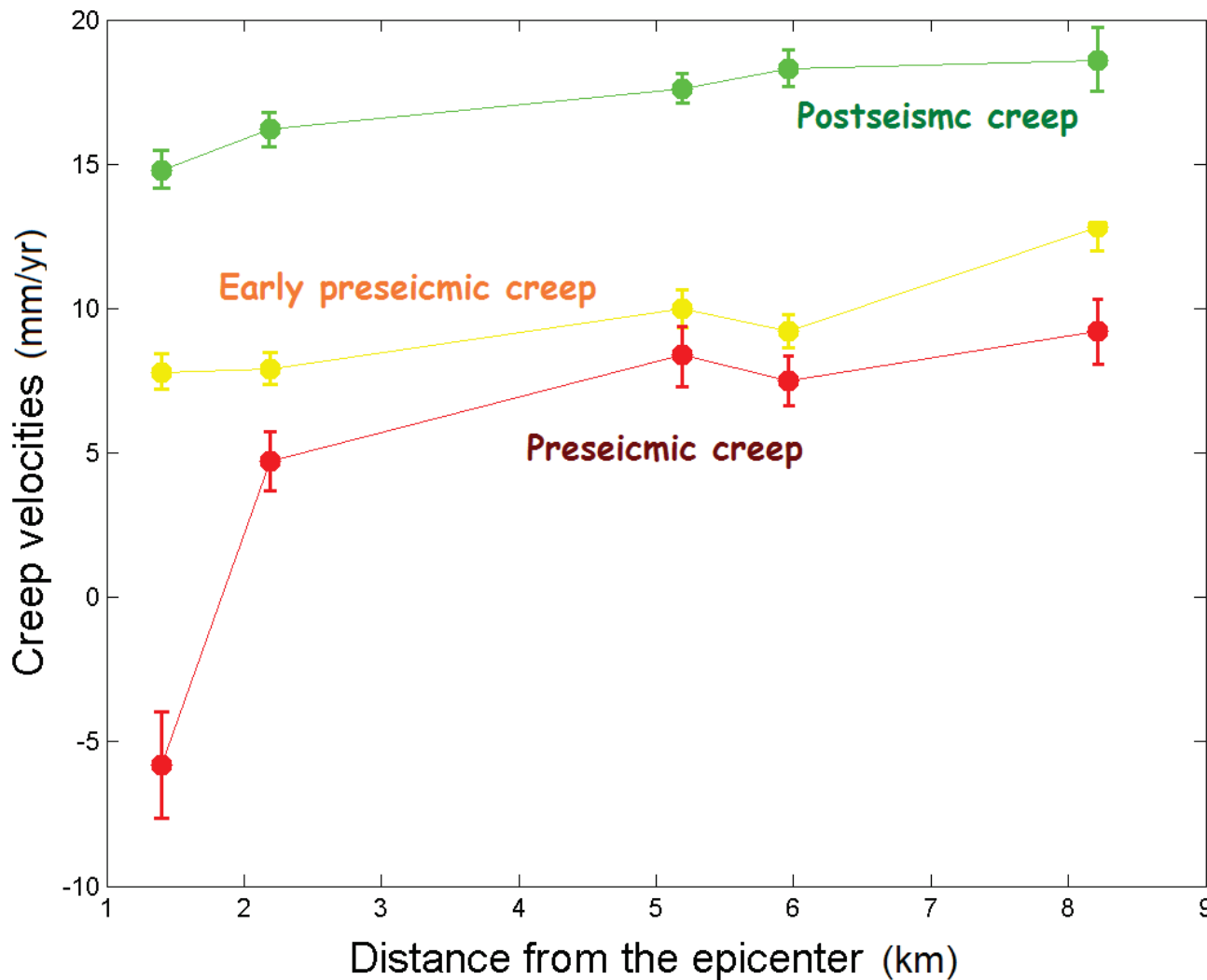
carh-hunt



masw-hunt

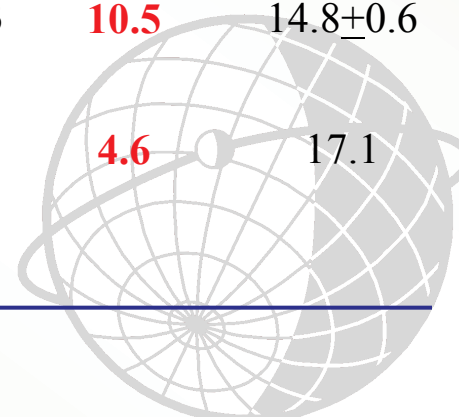


Creep velocities decreasing approaching to the epicenter

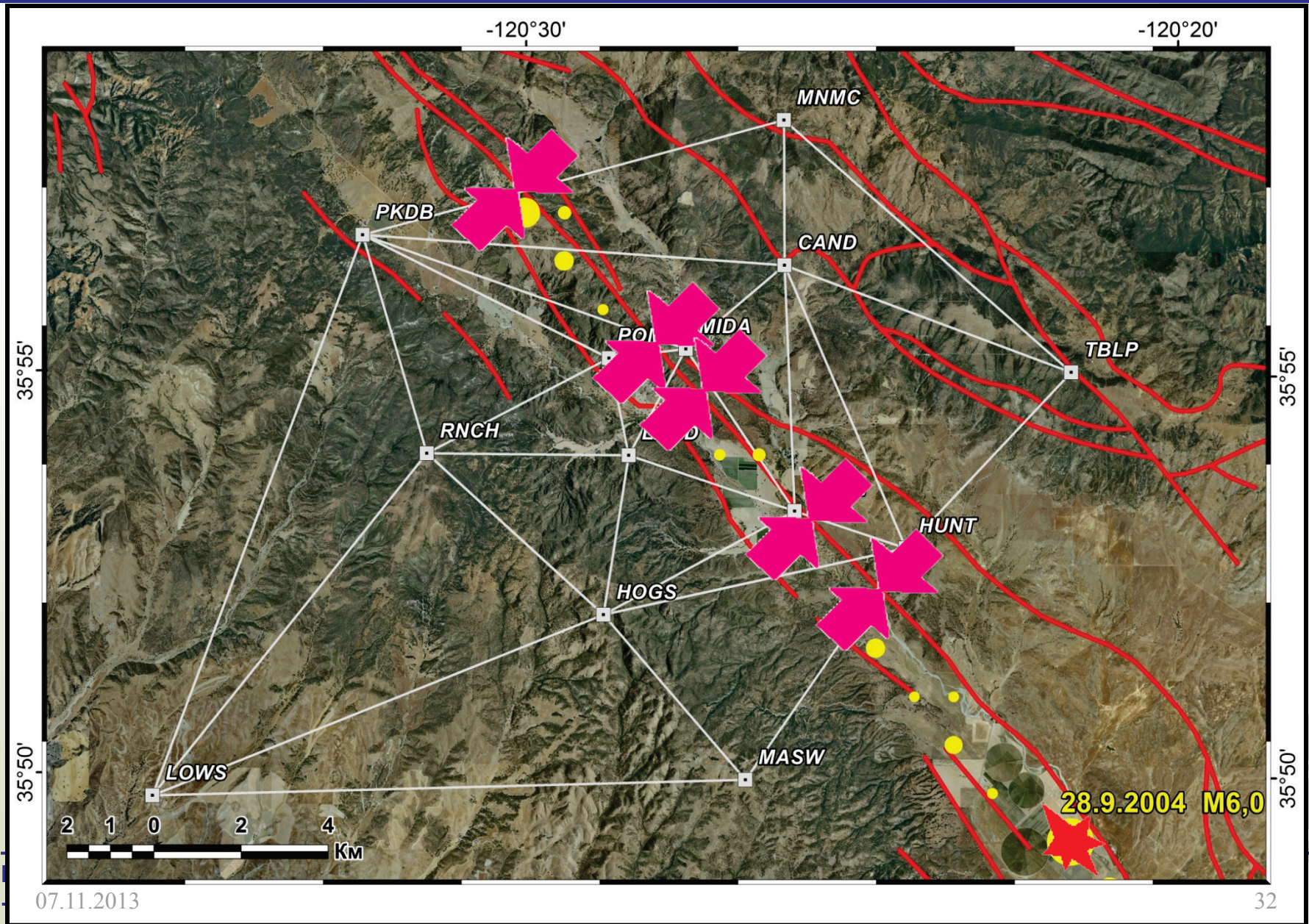


Creep changes from a north to a south of the network

Baseline	Creep change (jam) moment	Distance to the epicenter (km)	Jam rate km/yr	Earlier interval velocity (mm/yr)	Later interval velocity (mm/yr)	Δ_v/σ_Δ	t	Post seismic interval velocity (mm/yr)
pkdb-mnmc	2003.9	8210		12.8 ± 0.8	9.2 ± 1.1	3.6/1.0	3.6	18.6 ± 1.1
pomm-mida	2004.2	5963	7.5	9.2 ± 0.5	7.5 ± 0.8	1.7/0.7	2.4	18.3 ± 0.6
land-cand	2004.4	5192	6.0	10.0 ± 0.6	8.4 ± 1.1	1.6/0.7	2.3	17.6 ± 0.5
carh-hunt	2004.55	2193	9.3	7.9 ± 0.5	4.7 ± 1.0	3.2/0.8	4.0	16.2 ± 0.6
masw-hunt	2004.7	1400	8.5	7.8 ± 0.6	-5.8 ± 1.8	13.6/1.3	10.5	14.8 ± 0.6
Mean			7.8	9.5	7.4*			



Consecutive fault locking



Justification of elastic rebound model

- Creep velocity can be non zero just before an earthquake as it needs to be from the standard model?
- Creep velocity can be non stable months or years before an earthquake
- Creep velocity can decrease coming nearer to epicenter
- Creep velocity is about two times lower for pre- than post-seismic periods
- Elastic strain accumulation can begin not far from a previous earthquake



Concluding remarks

- 1) Presented results demonstrate geodetic capability for modeling of earthquake preparation and realization process.
- 2) Permanent GNSS observation can be effective for searching of locked or active zones of seismic active faults.
- 3) Creep analysis during permanent observation can provide evaluation of the risk of the next earthquake occurrence.

Thank you for attention

